Available online at www.sciencedirect.com
SCIENCE DIRECT®
Biochemical and Biophysical Research Communications 330 (2005) 163–171
BBRC
www.elsevier.com/locate/ybbrc

Raft-like membrane domains contain enzymatic activities involved in the synthesis of mammalian glycosylphosphatidylinositol anchor intermediates

Liza K. Pielsticker, Karl J. Mann, Wen-Lang Lin, Daniel Sevlever *

Department of Neuroscience, Mayo Clinic Jacksonville, Jacksonville, FL 32224, USA

Received 17 February 2005

Abstract

The synthesis of the glycosylphosphatidylinositol (GPI) anchor occurs in different compartments within the ER. We have previously shown that GPI anchor intermediates including GlcNAc-PI and GlcN-(acyl)PI are present in Triton insoluble membranes (TIMs), believed to be derived from lipid rafts. The present study was initiated to determine if GPI anchor intermediates move to raft-like domains after their synthesis or if these domains represent another ER compartment for GPI anchor synthesis. We determined that in transfected cells Pig-Ap and Pig-Lp, two proteins involved in the synthesis of GlcNAc-PI and GlcN-PI, respectively, are present in TIMs. In addition, we detected GlcNAc-PI synthase, GlcNAc-PI deacetylase, and GlcN-PI acyltransferase activities in TIMs isolated from untransfected cells. These results lend support to the possibility of additional GPI biosynthetic compartments in the ER and to the notion that GPI anchor intermediates produced in and outside raft-like domains may have a different fate.

Keywords: GPI; Lipid rafts; Membrane microdomains; Triton insoluble membranes

Glycosylphosphatidylinositol (GPI) anchors provide a stable association with the outer leaflet of the plasma membrane to a select group of mammalian proteins [1]. Among other properties the GPI anchor confers the attached proteins with the ability to partition in cellular membrane microdomains that are enriched in cholesterol and glycosphingolipids, commonly known as lipid rafts. These membrane domains are characterized by their resistance to solubilization by Triton X-100, and this property has been exploited to isolate rafts from cells as Triton insoluble membranes (TIMs) [2]. The presence of GPI-anchored proteins in lipid rafts is likely to have physiological relevance, since it is believed that some properties of GPI-anchored proteins, such as their ability to participate in signal transduction events [3] and to serve as receptors for bacterial toxins, depend on their localization in lipid rafts [4].

The synthesis of the GPI anchor starts in the cytoplasmic side and ends in the lumenal side of the endoplasmic reticulum (ER), where the transfer of the anchor to proteins occurs [5,6]. The first GPI biosynthetic step, which consists of the addition of *N*-acetylglucosamine (GlcNAc) to phosphatidylinositol (PI), is carried out by GPI-*N*-acetylglucosaminyl transferase (GPI-GnT). GPI–GnT is a complex that consists of at least six proteins: Pig-Ap, Pig-Cp, Pig-Hp, Gpi-1p, Pig-Pp, and Dpm2p [7], in which Pig-Ap is believed to be the catalytic component (see Fig. 1). Somatic mutations of the PIG-A gene result in defective GPI anchor synthesis in affected cells of patients suffering from the hemolytic disorder paroxysmal nocturnal hemoglobinuria [8]. Following GlcNAc transfer to phosphatidylinositol (PI), the pathway continues with the N-deacetylation

* Corresponding author. Fax: +1 904 953 7370.
E-mail address: sevlever.daniel@mayo.edu (D. Sevlever).

0006-291X/$ - see front matter © 2005 Elsevier Inc. All rights reserved.
doi:10.1016/j.bbrc.2005.02.136

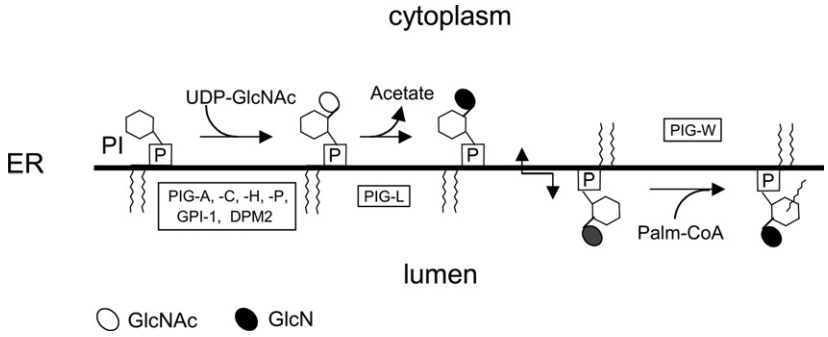

Fig. 1. Early steps of the mammalian GPI anchor biosynthetic pathway. The figure shows the steps and genes (inside the boxes) involved in the first three GPI biosynthetic reactions. The side of the ER membranes in which these reactions occur is also shown. PI, phosphatidylinositol.

of GlcNAc-PI to yield GlcN-PI, a reaction carried out by Pig-Lp [9,10]. The first two GPI anchor intermediates, GlcNAc-PI and GlcN-PI [11], and the catalytic domain of the proteins involved in their synthesis (i.e., Pig-Ap and Pig-Lp, respectively) [9,12] are accessible to probes in intact microsomes, strongly suggesting that up to this point the synthesis takes place on the cytoplasmic face of the ER (Fig. 1). PIG-W, the gene involved in the following step, i.e., palmitoylation of inositol in GlcN-PI to produce GlcN-(acyl)PI [13], has been recently cloned [14,15], and preliminary studies suggest that the acyl transfer occurs on the luminal side of the ER [15]. Therefore, it is likely that GlcN-PI is translocated across the ER membrane for acylation (Fig. 1). Subsequent mannosylation of GlcN-(acyl)PI, carried out by Pig-Mp [16], as well as the rest of the pathway, is thought to occur in the ER lumen based on the predicted topology of the enzymes [7].

In addition to the segregation of the GPI biosynthetic steps in both leaflets of the ER membrane, the pathway is likely to be segregated within the same leaflet of the membrane. Data from Stevens [17] and Menon [18] laboratories suggest that the first and second steps of the GPI anchor biosynthetic pathway, i.e., GlcNAc-PI synthesis and deacetylation, take place in different compartments within the ER.

GPI anchor intermediates (referred to in the text as GPIs) have also been found outside the ER in intracellular compartments that include the Golgi apparatus and at the plasma membrane, suggesting that these GPIs are produced in excess of anchoring needs [19]. The transport of GPIs to the plasma membrane has been shown to be blocked by conditions and reagents that perturb vesicular trafficking [20,21], indicating that this is the main mechanism by which GPIs reach the cell surface. This vesicular mechanism is also used by GPI-anchored proteins to travel through the secretory pathway.

The GPI anchor has been shown to be required for targeting GPI-anchored proteins to lipid rafts as they initiate their transit to the cell surface [22]. Therefore, it is not surprising that GPIs are also found concentrated in lipid rafts [23]. The localization of GPIs in lipid rafts is not restricted to the plasma membrane, since GPIs in the ER also partition in TIMs that share biophysical and compositional characteristics those of with lipid rafts [23]. Therefore, we assume that ER-TIMs are derived from raft-like membrane domains that exist in the ER.

The goal of this study was to determine whether GPIs move into raft-like domains after their synthesis as they travel to the cell surface or whether the synthesis of some GPIs in the ER occurs in raft-like domains. This latter possibility will support the proposal that a raft-like domain in the ER is one of the GPI biosynthetic compartments.

Materials and methods

Cells. HeLa S3 cells were from ATCC. G9PLAP.85 cells were a generous gift from Dr. Victoria Stevens (Emory University). These cells are defective in the synthesis of GPI-anchored proteins due to a mutation in the PIG-L gene and were derived from a parental CHO cell line (G9) that expresses placental alkaline phosphatase (PLAP) [24]. The 2A1 clone from HeLa cells stably transfected with GPI-PLD was obtained in our laboratory as previously reported [25].

Generation of PIG-L and PIG-A stable cell lines. pMEEB-FLAG-GST-PIG-A and pMEEB-PIG-L-GST-FLAG plasmids were a generous gift from Dr. Taroh Kinoshita (Osaka University), and details of their construction can be found elsewhere [9,12]. HeLa and G9PLAP.85 cells were plated in 6-well plates and the following day they were transfected with 1 μg pMEEB plasmids using Lipofectamine Plus reagent (Invitrogen) according to the recommendations of the manufacturer. After 48 h, the cells were transferred to 150 mm dishes and the following day selection of clones expressing Pig-Ap and Pig-Lp proteins was initiated by supplementing either DMEM for HeLa cells or F12-Ham's for G9PLAP.85 cells containing 10% of fetal calf serum, 100 i.u./ml penicillin, 100 μg/ml streptomycin, and 2 mM glutamine with 300 μg/ml hygromycin. Pig-Ap-HeLa clones were screened for FLAG-GST-tagged Pig-Ap by Western blot (see details in a section below). Clones of Pig-Lp-G9PLAP.85 transfectants were initially screened using an ELISA to detect the restoration of GPI-anchored PLAP activity, and Pig-Lp expression in PLAP positive clones was confirmed by Western blot.

Preparation of P10, P100, and microsomal membranes. Cells ($1–5 \times 10^8$) were washed twice with cold phosphate-buffered saline (PBS), resuspended in 10 ml buffer A (10 mM Hepes (pH 7.5) con-

taining 0.25 M sucrose and supplemented with 0.5 mM DTT, 0.1 mM TLCK, and 1 μg/ml leupeptin), and transferred to a nitrogen cavitation bomb (Kontes). The cells were held in the bomb at 450 psi for 30 min, and after cavitation they were treated with *Staphylococcus aureus* nuclease (30 U/ml) for 20 min on ice. Further cell disruption was achieved by passing the lysate three times through a 21-gauge needle. The lysate was clarified by centrifugation at 1000*g* for 10 min at 4 °C in a JA-20 rotor to remove large debris and nuclei. The resulting supernatant was centrifuged at 10,000*g* for 10 min at 4 °C in the same rotor. The pellet (P10) was collected and washed twice in 10 mM Hepes buffer (pH 7.5). The supernatant from the 10,000*g* spin was centrifuged at 100,000*g* for 1 h in a SW41 rotor to pellet the P100 fraction. P10 and P100 membranes were resuspended in 10 mM Hepes buffer (pH 7.5) for protein determination with a bicinchoninic acid (BCA) kit (Pierce). Approximately 16 mg of P10 and 18 mg of P100 were obtained from 2.5×10^8 cells. The membranes were either used immediately in in vitro labeling protocols or snap-frozen in liquid nitrogen and stored in 10% glycerol at −70 °C.

For microsomal preparation, the cells were incubated in culture medium supplemented with 5 μg/ml tunicamycin for 5 h before lysis. After washing with PBS, the cell pellet was resuspended in cold water (1 ml of water per 2×10^7 cells) supplemented with 0.1 mM TLCK and 1 μg/ml leupeptin, and vortexed for 1 min on ice. An equal volume 100 mM Hepes buffer (pH 7.5) supplemented with 50 mM KCl, 10 mM $MgCl_2$, 0.1 mM TLCK, and 1 μg/ml leupeptin was added. After mixing with vortexing, an aliquot of the lysates was taken for protein determination. Approximately 160 mg protein was obtained from 1.25×10^8 cells. The lysates were snap-frozen in liquid nitrogen and stored in 20% glycerol −70 °C. Before use in in vitro protocols, the lysates were thawed and microsomal membranes were obtained by pelleting for 20 min at 200,000*g* in a TLA-110 rotor.

Isolation of TIMs from cells and subcellular fractions. Cells ($0.5–1 \times 10^8$) were washed with PBS and resuspended in 1.5 ml buffer B (50 mM Hepes (pH 7.4) containing 0.15 M NaCl, 5 mM EDTA, and 1% Triton X-100, and supplemented with 1 μg/ml leupeptin, 1 μg/ml pepstatin, and 0.1 mM TLCK) on ice. In experiments using methyl-β-cyclodextrin, this cholesterol-binding agent was added to buffer B to a final concentration of 10 mM. All subsequent steps were carried out at 4 °C. The cells were lysed with 10 strokes in a manual tissue homogenizer and 3×5 s bursts (amplitude set at 20) in a microsonic cell disruptor (Kontes) over the course of 1 h. The homogenate was then centrifuged for 3 min at 2500*g* to pellet unbroken cells and large insoluble material. The supernatant of the low-speed centrifugation (~1 ml) was mixed with an equal volume of 80% sucrose and placed at the bottom of a 12-ml centrifuge tube, and a discontinuous sucrose gradient was formed by overlaying 6 ml of 38% sucrose and 3 ml of 5% sucrose. After 19 h of centrifugation in a SW41 rotor at 230,000*g*, 1-ml fractions were collected from the top. TIMs floated to the interface between 5% and 38% sucrose, and appeared as an opalescent band. For TIM isolation from P10 and P100, these membranes were incubated for 1 h with buffer B at 4 °C, followed by floatation in a sucrose gradient as described above.

For in vitro labeling experiments, TIMs isolated from cells or from P10 and P100 membranes were pelleted after dilution of the sucrose with 50 mM Hepes buffer (pH 7.4) supplemented with proteinase inhibitors and centrifugation for 2 h at 230,000*g* in a SW41 rotor. After protein determination, the membranes were either used immediately or stored in 10% glycerol at −70 °C. TIMs did not lose activity even after repeated cycles of freezing and thawing. The protocol to isolate TIMs from cells yielded between 0.8 and 1.0 mg of membranes.

UDP-[^{3}H]GlcNAc labeling of membranes. The synthesis of GlcNAc-PI, GlcN-PI, and GlcN-(acyl)PI in membranes was assessed using a previously reported protocol [26]. Subcellular membranes and TIMs were labeled with 2 or 5 μCi UDP-[^{3}H]GlcNAc (ARC) for 1 h at 37 °C in 150 μl of 50 mM Hepes buffer (pH 7.5) containing 5 mM $MgCl_2$, 0.5 mM DTT, 1 μg/ml leupeptin, 0.1 mM TLCK, 0.2 μg/ml tunicamycin, 1 mM ATP, 1 mM GTP, 1 μM CoA, and 1 mM 2,3-dimercapto-1-propanol. Radiolabeled lipid species were extracted by addition of 650 μl water and 3 ml chloroform/methanol (1:2) containing 0.1 M HCl to make a single phase chloroform/methanol/water (3:6:0.8) and vortexed for 2 min. To obtain an organic and aqueous phase, 1 ml of water and 1 ml of chloroform were added. After 3 min of vortexing, the upper aqueous phase was removed and the organic phase was extracted once more with an equal volume of a pre-equilibrated aqueous phase. The radiolabeled lipids present in the organic phase were analyzed by TLC using chloroform/methanol/1 N NH_4OH as the developing solvent.

Western blot analysis of sucrose gradient fractions. Clones of Pig-Ap-HeLa and Pig-Lp-G9PLAP.85 transfectants were lysed in buffer B and 12 1-ml fractions from the sucrose gradient were obtained. The sucrose fractions were brought to 4 ml using Tris–HCl-buffered saline (TBS) to obtain a final concentration of 10 mM Tris–HCl (pH 7.4) and 150 mM NaCl, and were supplemented with 1% NP-40, 1 mM EDTA, 1 μg/ml of leupeptin and pepstatin, and 0.1 mM TLCK (TBS-NP-40 buffer). Anti-FLAG M2 (Sigma) agarose beads (30 μl) were pre-equilibrated and washed three times in the same buffer before overnight incubation with the sucrose fractions in a shaker at 4 °C. The following day the beads were collected by centrifugation and washed three times with TBS-NP-40 buffer. The material bound to the anti-FLAG M2 beads was eluted either by boiling the beads in SDS–PAGE loading buffer or with 200 μg/ml of FLAG peptide (Sigma) for 2 h in a shaker at room temperature. After transferred to PVDF membranes, the blots were first incubated with a rabbit polyclonal anti-FLAG antibody (Sigma) and then with a horseradish peroxidase-conjugated anti-rabbit antibody. FLAG-tagged proteins were detected with ECL (Amersham) reagent.

Electron microscopy. TIM pellets (10 μg) obtained as described in the previous section were fixed in 1.5% glutaraldehyde in 0.1 M cacodylate buffer (pH 7.4) containing 1% $CaCl_2$, then postfixed in 1% OsO_4 in water, dehydrated in ethanol, infiltrated, and embedded in Epon 812 (Polysciences, Warrington, PA). Ultrathin sections were stained with uranyl acetate and lead citrate, and examined with a Philips 208S electron microscope as described in [27].

Results and discussion

GPI-GnT and GlcNAc-PI deacetylase are present in TIMs

To investigate the presence in raft-like domains of gene products involved in the synthesis of GlcNAc-PI and GlcN-PI, we generated stable cell lines expressing FLAG- and GST-tagged versions of PIG-A and PIG-L genes. For the analysis of Pig-A protein (Pig-Ap), we transfected HeLa S3 cells and for studies involving Pig-Lp we transfected G9PLAP.85 cells, a GPI anchor negative CHO mutant defective in PIG-L [24]. Transfection of PIG-L restored the synthesis of GPI-anchored PLAP in G9PLAP.85 cells (data not shown), indicating that Pig-Lp was targeted to the ER. Analysis of the subcellular distribution of Pig-proteins expressed using the same vectors employed in this study also showed that these proteins remained preferentially in the ER [9,12].

Raft localization of Pig-Ap and Pig-Lp was assessed in several clones from Pig-Ap-HeLa and Pig-Lp-G9PLAP.85 transfectants by establishing the presence of these proteins in TIMs. TIMs have been proposed to be largely derived from lipid rafts, membrane

domains that exist in cells [28]. TIMs were prepared using a widely accepted protocol that involves cell lysis with Triton X-100 and floatation of the lysates to equilibrium in a sucrose gradient. Under these conditions TIMs tend to float close to the top of the gradient, usually between fractions 3 and 5. Twelve gradient fractions from Pig-Ap-HeLa and Pig-Lp-G9PLAP.85 cell lysates were collected starting from the top of the gradient and they were incubated with beads coated with anti-FLAG antibody to isolate FLAG-tagged Pig-Ap and Pig-Lp. The material captured by the beads was eluted with FLAG peptide and analyzed by Western blot using anti-FLAG antibodies. Blots of the distribution of Pig-Ap and Pig-Lp in the sucrose gradients from representative Pig-Ap-HeLa and Pig-Lp-G9PLAP.85 clones showed the presence of both proteins in TIM fractions (3–5) (Figs. 2A and B). The percentage of Pig-Lp in TIMs (calculated using fractions 3–5 of the sucrose gradient as TIMs and fractions 9–11 as non-TIM fractions) was about 23%. For Pig-Ap that percentage was slightly but consistently higher, around 34%. Therefore, it appears that the majority of the Pig-Ap and Pig-Lp are located outside TIMs in the ER. Since the efficiency of Triton or any other detergent to extract rafts from cells is not known, we cannot conclude that most Pig-Ap and Pig-Lp reside in non-raft-like domains in the ER.

Analysis of the supernatants of each fraction after immunoprecipitation showed that most of the FLAG-tagged proteins were captured by the beads and that the efficiency of the capture was the same for all the gradient fractions (data not shown). Furthermore, the distribution of Pig-Ap and Pig-Lp in the sucrose gradient was not skewed by immunoprecipitation with anti-FLAG beads, since Western blot analysis of the fractions without the immunoprecipitation step produced a similar distribution of Pig-Ap and Pig-Lp in TIMs (data not shown).

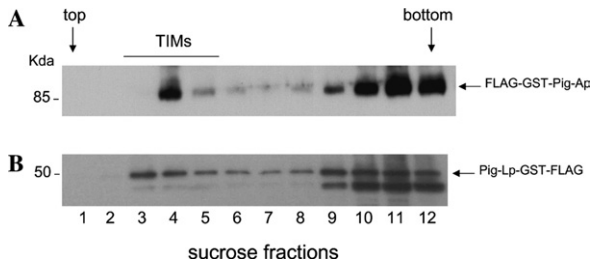

Fig. 2. Distribution of Pig-Ap and Pig-Lp in sucrose gradients. Pig-Ap-HeLa and Pig-Lp-G9PLAP.85 transfectants were lysed in buffer B (see Materials and methods), sucrose gradient fractions were obtained and incubated with anti-FLAG M2 beads. The material retained on the beads was eluted with FLAG peptide, the eluate was concentrated in a Speed-Vac, and the proteins were resolved by SDS–PAGE. Pig-Ap (A) and Pig-Lp (B) in each sucrose fraction, migrating at the expected MW (after considering the contributions of the FLAG and GST tags), were detected by Western blot using a polyclonal anti-FLAG antibody and ECL as developing reagent. The nature of the additional band present in the non-TIMs fractions in (B) is unknown. The position of sucrose gradient fractions containing TIMs is indicated.

Pig-Ap is an ER transmembrane protein with a large amino-terminal domain that includes the putative catalytic domain on the cytoplasmic side of the ER and a small carboxy-terminal domain in the ER lumen [29]. Pig-Lp is also a transmembrane protein but in contrast to Pig-Ap has a reverse orientation on the ER [30]. Sequence analysis of Pig-Ap did not provide any clue as to the way in which the protein is targeted to TIMs. Similar analysis of Pig-Lp showed the presence of a cysteine residue (Cys-75) that has the potential to be modified by palmitic acid [30]. Palmitoylation is a posttranscriptional modification that has been shown to target proteins to TIMs [31].

GlcNAc-PI, GlcN-PI, and GlcN-(acyl)PI can be synthesized in isolated TIMs

Having established the presence of Pig-Ap and Pig-Lp in TIMs, we next asked whether the TIM pool of these proteins is able to synthesize GlcNAc-PI and GlcN-PI. Detection of GPI biosynthetic activities in various membrane fractions such as cell lysates, microsomes, and ER membranes using radiolabeling protocols is well documented [13,32–34]. In these protocols, the membrane fractions are the source of the GPI biosynthetic enzymes as well as the substrates.

The enzymatic activities of Pig-Ap and Pig-Lp were assayed using TIMs from untransfected cells to rule out the possibility that the presence of the tagged-Pig-Ap and -Pig-Lp in TIMs isolated from transfectants is caused by the transfection and does not reflect the distribution of the endogenous proteins. TIMs from HeLa cells were prepared as described for the analysis of Pig-Ap and Pig-Lp, and were isolated by pooling TIM fractions (3–5) from the sucrose gradient and pelleting them by centrifugation at 230,000*g* after dilution of the sucrose. Purified TIMs were then labeled with 2.5 μCi UDP-[^{3}H]GlcNAc at 37 °C in labeling buffer and the reaction products were analyzed at 30 min, 60 min, 90 min, 4 h, and 17 h.

Stevens and Zhang [26] showed that addition of CoA to UDP-[^{3}H]GlcNAc labeling reactions greatly stimulates the synthesis of GlcN-(acyl)PI (see Fig. 1). Thus, the reaction mixtures were supplemented with CoA to determine if, in addition to GPI-GnT and GlcNAc-PI deacetylase, GlcN-PI palmitoyltransferase activity (responsible for the formation of GlcN-(acyl)PI) is also present in TIMs. For this analysis, radiolabeled lipid species were extracted with a mixture of chloroform/methanol/water at the above-indicated time points, and after phase separation, the lipids recovered in the organic phase were resolved by TLC. ^{3}H-labeled GlcNAc-PI, GlcN-PI, and GlcN-(acyl)PI standards were run alongside to identify these species in TIMs. The

identities of GlcNAc-PI and GlcN-PI were further confirmed by their susceptibility to bacterial PI-PLC and by treatment with acetic anhydride to *N*-acetylate GlcN-PI [35], which caused the conversion of GlcN-PI to GlcNAc-PI (data not shown). The synthesis of the three main lipid species identified in TIMs: GlcNAc-PI, GlcN-PI, and GlcN-(acyl)PI increased linearly with time during the first 4 h of incubation and reached a plateau afterwards (Figs. 3A and B).

We then tested different amounts of TIMs ranging from 50 to 800 μg in a 1-h radiolabeling protocol.

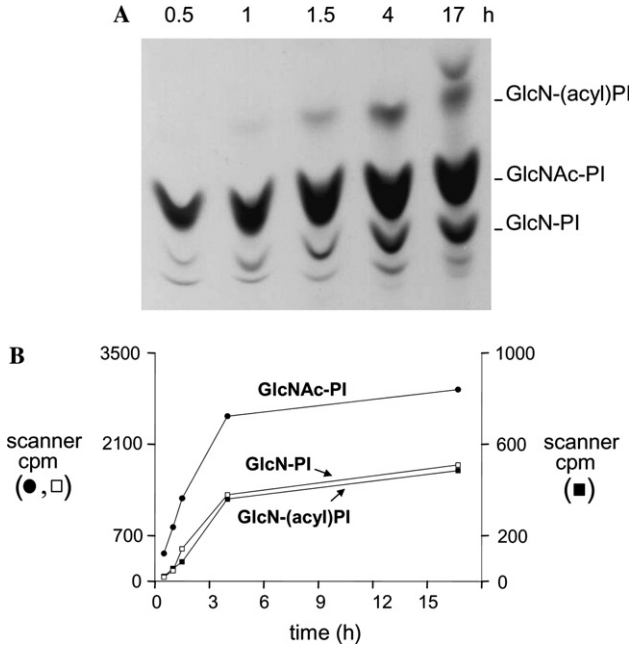

Fig. 3. Kinetics of GPI synthesis in TIMs. Membranes (200 μg) were incubated with 2.5 μCi of UDP-[^{3}H]GlcNAc for the indicated amount of time. At the end of the incubation, the radiolabeled lipids were extracted and analyzed on TLC using chloroform/methanol/1 N NH_4OH as the developing solvent. (A) Fluorography of TLC plate after spraying with EN^{3}HANCE (Amersham). (B) Quantitation of the GcNAc-PI (closed circles), GlcN-PI (open squares), and GlcN-(acyl)PI (closed squares) was performed using software provided with a Bioscan TLC scanner.

Quantitative TLC analysis of the products showed that the incorporation of ^{3}H into GlcNAc-PI and GlcN-PI increased proportionally to the amount of TIMs up to 200 μg. No further incorporation of ^{3}H into GPIs was observed when more than 200 μg of TIMs were used in the reactions (data not shown). In summary, the above experiments showed that the synthesis of GlcNAc-PI, GlcN-PI, and GlcN-(acyl)PI in TIMs was time- and concentration-dependent.

Deacetylation of GlcNAc-PI in TIMs

The following experiments were focused on the conversion of GlcNAc-PI to GlcN-PI in TIMs. Since microsomes are the most commonly used membrane fraction in experiments assessing the synthesis of early GPIs, these membranes were assayed in parallel reactions with TIMs. 200 μg of both microsomes and TIMs from HeLa S3 cells was labeled with UDP-[^{3}H]GlcNAc at 37 °C for 1 h. TIMs from 2A1 cells, a clone of HeLa cells stably transfected with GPI-PLD [25], an enzyme specific for GPI structures, were also labeled in parallel. After 1 h one-third of each reaction was extracted as described previously. The counts in the organic phase were consistently higher in TIMs (~50%) than in microsomes. The increased incorporation of ^{3}H into lipids in TIMs was probably due to lower levels of UDP-GlcNAc degrading activity in TIMs, since TLC analysis of the aqueous phases showed the presence of UDP-[^{3}H]GlcNAc degradation products in the microsomal but not in the TIM samples (data not shown). TLC analysis of the organic phase after 1 h incubation indicated that similar amounts of GlcNAc-PI and GlcN-PI were generated in microsomes, in contrast to TIMs from HeLa cells (S3 and 2A1) that produced large amounts of GlcNAc-PI and relatively low levels of GlcN-PI (Fig. 4). Quantitation of GlcNAc-PI and GlcN-PI in microsomes and in TIMs indicated a ratio of ~1.5 and ~4.5, respectively, suggesting that deacetylation of GlcNAc-PI in microsomes is achieved more readily than in TIMs.

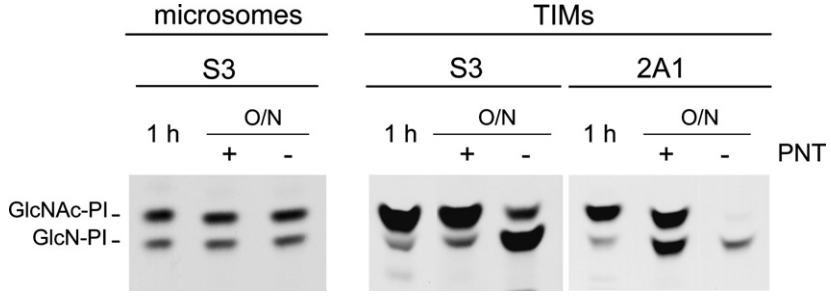

Fig. 4. Deacetylation of GlcNAc-PI in TIMs. Microsomes and TIMs from HeLa S3 and TIMs from 2A1 cells were labeled for 1 h with 5 μCi UDP-[^{3}H]GlcNAc. The unincorporated UDP-[^{3}H]GlcNAc was removed after dilution of the reaction mixtures and pelleting the membranes for 1 h at 100,000*g*. The pellet was divided into three aliquots, one was directly extracted to obtain GPIs and the other two were incubated overnight at 37 °C in GPI-PLD buffer (see Materials and methods) supplemented with (+) and without (−) phenanthroline (PNT). Radiolabeled GPIs generated after 1 h and overnight incubations were analyzed on TLC.

Although the higher GPI-GnT activity observed in TIMs could be due to an enrichment of PI in TIMs compared to microsomes, this possibility seems unlikely since we have previously shown that PI is mostly excluded from TIMs [23]. Still, it is possible that TIMs are enriched in a minor PI pool that acts as acceptor for GlcNAc. Pig-Ap is the catalytic component of the GPI–GnT complex and, as mentioned in the Introduction, Pig-Cp, Pig-Hp, Gpi-1p, Pig-Pp, and Dpm2p are the other components of this complex. Since Pig-Cp, Pig-H, and Pig-Pp are essential for GPI-GnT activity [7], it is reasonable to assume that these three proteins are also present in TIMs.

To determine if further deacetylation of GlcNAc-PI can be achieved in TIMs, the remaining two-thirds of TIMs and microsomes that were labeled for 1 h were pelleted at 100,000*g* and incubated overnight at 37 °C. We reasoned that TIMs from 2A1 cells that contain GPI-PLD activity [25] would be particularly useful to further confirm the identities of the labeled species in TIMs, since GPI-PLD has been shown to cleave GlcN-PI but not GlcNAc-PI [35,36]. Therefore, for the overnight incubation, 1-h labeled microsomes and TIMs were resuspended in GPI-PLD buffer (50 mM Mes (pH 6.5) containing 0.05% Triton X-100 and 0.1 mM $CaCl_2$) in the absence and presence of 500 μM phenanthroline (PNT). PNT was included in the reactions to inhibit GPI-PLD as we previously reported [25] and GlcNAc-PI deacetylase, since the activity of this enzyme was reported to be stimulated by many divalent cations including transition metals [10]. TLC analysis of the organic phases revealed no differences between PNT-treated and -untreated HeLa microsomes (Fig. 4). In TIMs from HeLa S3 and 2A1 cells, however, GlcNAc-PI was converted to GlcN-PI in the absence of PNT and this conversion was prevented when this chelator was present (Fig. 4). The PNT inhibition of GlcN-PI deacetylase is likely due to chelation of transition metals, which are probably present in trace amounts in TIMs. In TIMs isolated from 2A1 cells, GlcNAc-PI was partially (~30%) converted to GlcN-PI, even in the presence of PNT. In contrast, in the absence of PNT, most of the counts were not retained in the organic phase and only a very faint band corresponding to GlcN-PI was left (Fig. 4). This was probably the result of two activities present in 2A1 TIMs: GlcNAc-PI deacetylase that generated GlcN-PI and GPI-PLD that subsequently cleaved it. These results demonstrated that complete deacetylation of GlcNAc-PI can be achieved in TIMs. Experiments designed to assess the contribution of Triton X-100 and Ca^{2+} (present in the GPI-PLD buffer) to the deacetylation of GlcNAc-PI in TIMs showed that both compounds stimulated GlcNAc-PI deacetylation to a similar extent. Furthermore, Triton X-100 and Ca^{2+} do not appear to have a synergistic effect on the deacetylation of GlcNAc-PI (data not shown).

Data from Stevens and Menon laboratories suggested that GPI anchor biosynthetic activities are not uniformly distributed in the ER. Both laboratories showed that the formation of GlcNAc-PI and GlcN-PI occurs in different membranes within the ER [17,18], and Menon laboratory proposed that GlcN-PI synthesis takes place in an ER region that is associated with the mitochondria [18]. These mitochondria associated membranes (MAMs) are contained in a subcellular fraction that pellets at 10,000*g* (P10) [18]. Therefore, we investigated whether TIMs isolated from a P10 fraction (P10-TIMs) have a higher GlcNAc-PI deacetylase activity than TIMs obtained from heavier membranes that pellet at 100,000*g* (P100) and contain ER membranes. For that purpose, P10 and P100 fractions were prepared according to Vidugiriene et al. [18] and TIMs isolated from these membranes. The yield of TIMs from both P10 and P100 membranes was low. P10-TIMs were below the detection levels of the protein determination assay and only 10 μg P100-TIMs was obtained. Unfractionated P10 and P100 membranes, and TIMs from these fractions were labeled in parallel with UDP-[^{3}H]GlcNAc. TLC analysis of the radiolabeled lipids in unfractionated (unf. in Fig. 5) P10 and P100 membranes showed a relative enrichment of GlcN-PI in P10 membranes (Fig. 5A). In contrast, TIMs from both membrane fractions have a similar lipid profile (Fig. 5A).

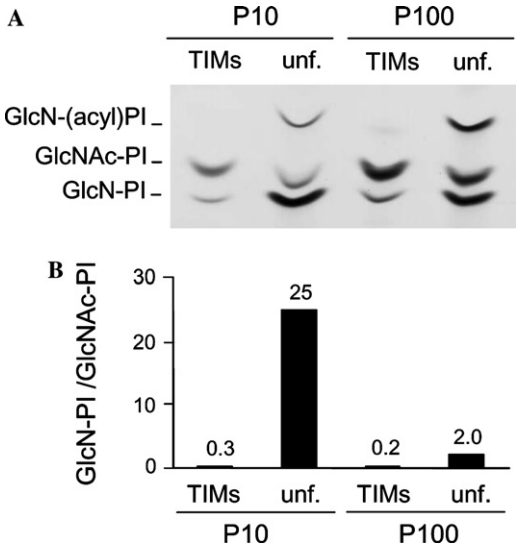

Fig. 5. Comparison of GlcNAc-PI deacetylation in TIMs derived from P10 and P100 membranes. P10 and P100 membranes (15.7 and 17.4 mg, respectively) were obtained and fourth-fifths were incubated in buffer B for 1 h and floated in a sucrose gradient to produce TIMs. Isolated P10- and P100-TIMs, and one-fifth of the unfractioned (unf. in the figure) P10 and P100 membranes were labeled for 1 h with 2.5 μCi UDP-[^{3}H]GlcNAc. After extraction of the GPIs, aliquots of organic phase of the unfractioned P10 and P100 reactions (equivalent to ~1 mg of membranes) and the whole organic phase of the P10- and P100-TIM samples were analyzed on TLC.

The weaker GlcNAc-PI and GlcN-PI signals observed in P10-TIMs as compared to P100-TIMs are likely to result from the lower yield of TIMs from P10 membranes. Quantitative analysis of the GlcN-PI to GlcNAc-PI ratio showed that TIMs from both membrane fractions have a similar ratio (0.3 and 0.2) despite the fact that the relative level of GlcN-PI in P10 membranes was almost 10 times higher than in P100 membranes (Fig. 5B). Therefore, it is likely that the GlcNAc-PI deacetylase activity detected in TIMs is not derived from MAMs. A straight interpretation of the altered GlcN-PI to GlcNAc-PI ratio observed in P10- and P100-TIMs when compared to the unfractionated membranes suggests that GlcNAc-PI deacetylase is underrepresented in TIMs. However, it is possible that topological and/or compositional rearrangements of the ER membranes that occur during TIM preparation provide an unfavorable environment for GlcNAc-PI deacetylation. This possibility appears to be supported by the fact that after overnight incubation in GPI-PLD buffer (containing detergent), complete conversion of the GlcNAc-PI generated in TIMs can be accomplished. The results of the experiment described in the following section further support the above mentioned possibility. In conclusion, we believe that TIMs are not one of the compartments in which differential GPI-GnT and GlcN-PI deacetylase activities have been reported [17,18]. Significantly, a recent report from Menon laboratory showed that in HeLa cells (the same cell line used in the above-described studies), GlcNAc-PI deacetylase activity is equally distributed between the ER and MAMs [30].

Effect of MCD on GlcNAc-PI deacetylation in TIMs

To investigate the role of cholesterol in the synthesis of GPIs in TIMs, methyl-β-cyclodextrin (MCD), a cholesterol-binding molecule, was included in the lysis buffer during TIM isolation. This approach differed from the more commonly used protocol of treating intact cells with MCD before TIM isolation. However, this strategy was chosen because we presumed that intracellular TIMs (like ER-TIMs) would not be affected by MCD treatment of intact cells. TIMs isolated in the presence and absence of MCD were assayed for GPI synthesis using the UDP-[^{3}H]GlcNAc labeling protocol described above. MCD facilitated the conversion of GlcNAc-PI to GlcN-PI and greatly stimulated the subsequent generation of GlcN-(acyl)PI (Fig. 6, compare lanes 1 and 3 in A). In the absence of MCD, the ratio of GlcN-PI to GlcNAc-PI in TIMs was 0.12 ± 0.04. In contrast, when TIMs were prepared in the presence of MCD the ratio was approximately eight times higher, 1.0 ± 0.2. In addition, GlcN-(acyl)PI was almost four times higher in MCD-treated TIMs. To determine if the MCD effect was due to stimulation of GlcNAc-PI deacetylase, the experiment was repeated in the presence of EDTA. As

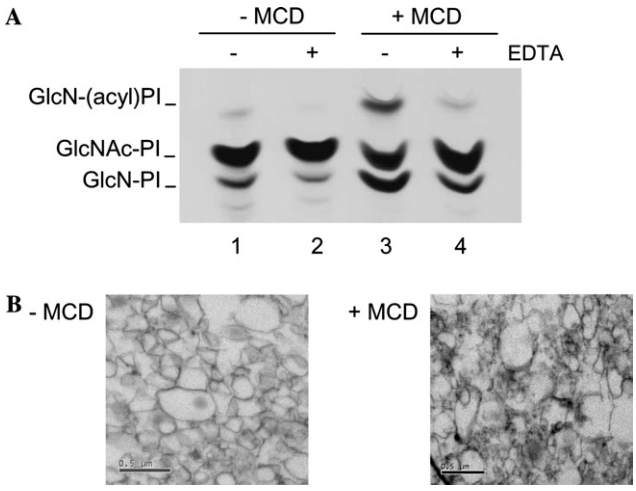

Fig. 6. Effect of methyl-β-cyclodextrin on the deacetylation of GlcNAc-PI in TIMs. (A) Membranes (120 μg) obtained in the presence and absence of 10 mM β-methyl cyclodextrin (MCD) were incubated for 1 h with 2.5 μCi UDP-[^{3}H]GlcNAc. MCD-treated and -untreated samples were supplemented with (+) and without (−) 5 mM EDTA. (B) MCD-treated and -untreated TIMs (10 μg) were fixed and prepared for EM imaging as described in Materials and methods.

mentioned previously, GlcNAc-PI deacetylase is dependent on divalent cations, and EDTA was added to sequester Mg^{2+} present in the labeling buffer. The stimulation of GlcN-PI and GlcN-(acyl)PI syntheses by MCD was substantially blocked when EDTA was present in the reaction (Fig. 6, lanes 2 and 4 in A).

The increase in GlcNAc-PI deacetylase activity with MCD was unexpected, since MCD is commonly used to disrupt TIMs. However, it has been reported that certain TIM components are not released from these membranes after MCD treatment [37]. Under our experimental conditions we did not observe any significant differences in the yield of TIMs (measured by protein determination) isolated in the presence and absence of MCD. Nevertheless, we were able to observe MCD effects on TIM vesicle morphology in electron microscope (EM) images. EM images of MCD-treated TIMs showed a more heterogeneous vesicular composition than in the untreated TIM controls (Fig. 6B).

The increase in GlcNAc-PI deacetylase activity can be explained by proposing that GlcNAc-PI deacetylase is more efficiently recovered in TIMs prepared in the presence of MCD. We tested this possibility using Pig-Lp-G9PLAP.85 to establish the distribution of Pig-Lp in TIMs isolated in the presence and absence of MCD but found no significant changes (data not shown); therefore, we discarded this possibility. Other explanations for the MCD effect in TIMs are that MCD facilitates the coupling of the synthesis and deacetylation of GlcNAc-PI or that either cholesterol or another factor removed by MCD inhibits GlcNAc-PI deacetylase. The former possibility appears to be supported by the

more disorganized morphology seen in EM images of MCD-treated samples (Fig. 6B) that could favor the interaction between GlcNAc-PI deacetylase and its substrate.

Conclusions

We have demonstrated that GPI–GnT, GlcNAc-PI deacetylase, and GlcN-PI acyltransferase are present in TIMs. Since all the GPI biosynthetic activities have been shown to be confined to the ER [7] and TIMs are derived from rafts that exist in cells, we propose that GPI–GnT, GlcNAc-PI deacetylase, and GlcN-PI acyltransferase are present in raft-like domains in the ER. Unfortunately, limitations of the existing protocols to isolate rafts either as TIMs or using detergent-free methods preclude any reliable estimation of the amount of GPI biosynthetic activities present in raft-like domains. To our knowledge this is the first report documenting the presence of biosynthetic activities in ER-TIMs that have raft-like properties. Interestingly, we found ER proteins oriented toward both sides (cytoplasmic and lumenal) of the membrane in TIMs in the ER, suggesting that this type of membrane domains is not restricted to a particular leaflet of the ER membrane.

Finally, due to the proposed involvement of lipid rafts in intracellular trafficking, it is tempting to speculate that the GPI pool synthesized in raft-like domains in the ER is destined to the plasma membrane and is probably not involved in protein anchoring.

Acknowledgments

This work was supported by NIH Grant DK55002 to D.S. We thank Dr. Terry Rosenberry and M. Sevlever for careful reading of the manuscript.

References

[1] M.A. Ferguson, The structure, biosynthesis and functions of glycosylphosphatidylinositol anchors, and the contributions of trypanosome research, J. Cell Sci. 112 (1999) 2799–2809.
[2] D.A. Brown, E. London, Functions of lipid rafts in biological membranes, Annu. Rev. Cell. Dev. Biol. 14 (1998) 111–136.
[3] K. Simons, D. Toomre, Lipid rafts and signal transduction, Nat. Rev. 1 (2000) 31–39.
[4] L. Abrami, M. Fivaz, P.E. Glauser, R.G. Parton, F.G. van der Goot, A pore-forming toxin interacts with a GPI-anchored protein and causes vacuolation of the endoplasmic reticulum, J. Cell Biol. 140 (1998) 525–540.
[5] V. Stevens, Biosynthesis of glycosylphosphatidylinositol membrane anchors, Biochem. J. 310 (1995) 361–370.
[6] D. Sevlever, R. Chen, M.E. Medof, Synthesis of the GPI anchor, in: N.S. Young, J. Moss (Eds.), PNH and GPI-linked Proteins, Academic Press, New York, 2000, pp. 199–220.
[7] T. Kinoshita, N. Inoue, Dissecting and manipulating the pathway for glycosylphosphatidylinositol-anchor biosynthesis, Curr. Opin. Chem. Biol. 4 (2000) 632–638.
[8] J. Takeda, T. Miyata, K. Kawagoe, Y. Iida, Y. Endo, T. Fujita, M. Takahashi, T. Kitani, T. Kinoshita, Deficiency of the GPI anchor caused by a somatic mutation of the PIG-A gene in paroxysmal nocturnal hemoglobinuria, Cell 73 (1993) 703–711.
[9] N. Nakamura, N. Inoue, R. Watanabe, M. Takahashi, J. Takeda, V.L. Stevens, T. Kinoshita, Expression cloning of PIG-L, a candidate *N*-acetyl-glucosaminyl-phosphatidylinositol deacetylase, J. Biol. Chem. 272 (1997) 15834–15840.
[10] R. Watanabe, K. Ohishi, Y. Maeda, N. Nakamura, T. Kinoshita, Mammalian PIG-L and its yeast homologue Gpi12p are *N*-acetylglucosaminylphosphatidylinositol de-*N*-acetylases essential in glycosylphosphatidyl-inositol biosynthesis, Biochem. J. 339 (1999) 185–192.
[11] J. Vidugiriene, A.K. Menon, Early lipid intermediates in glycosylphosphatidylinositol anchor assembly are synthesized in the ER and located in the cytoplasmic leaflet of the ER membrane bilayer, J. Cell Biol. 121 (1993) 987–996.
[12] R. Watanabe, T. Kinoshita, R. Masaki, A. Yamamoto, J. Takeda, N. Inoue, PIG-A and PIG-H which participate in the glycosylphosphatidylinositol anchor biosynthesis, form a protein complex in the endoplasmic reticulum, J. Biol. Chem. 271 (1996) 26868–26875.
[13] M. Urakaze, T. Kamitani, R. DeGasperi, E. Sugiyama, H.-M. Chang, C.D. Warren, E.T.H. Yeh, Identification of a missing link in glycosyl-phosphatidylinositol anchor biosynthesis in mammalian cells, J. Biol. Chem. 267 (1992) 6459–6462.
[14] M. Umemura, M. Okamoto, K.-i. Nakayama, K. Sagane, K. Tsukahara, K. Hata, Y. Jigami, GWT1 gene is required for inositol acylation of glycosylphosphatidylinositol anchors in yeast, J. Biol. Chem. 278 (2003) 23639–23647.
[15] Y. Murakami, U. Siripanyapinyo, Y. Hong, J. Young Kang, S. Ishihara, H. Nakakuma, Y. Maeda, T. Kinoshita, PIG-W is critical for inositol acylation but not for flipping of glycosylphosphatidylinositol-anchor, Mol. Biol. Cell 14 (2003) 4285–4295.
[16] Y. Maeda, R. Watanabe, C.L. Harris, Y. Hong, K. Ohishi, K. Kinoshita, T. Kinoshita, PIG-M transfers the first mannose to glycosylphosphatidyl-inositol on the lumenal side of the ER, EMBO J. 20 (2001) 250–261.
[17] V.L. Stevens, H. Zhang, E.S. Kristyanne, Stimulation of glycosylphosphatidylinositol biosynthesis in mammalian cell-free systems by GTP hydrolysis: evidence for the involvement of membrane fusion, Biochem. J. 341 (1999) 577–584.
[18] J. Vidugiriene, D.K. Sharma, T.K. Smith, N.A. Baumann, A.K. Menon, Segregation of glycosylphosphatidylinositol biosynthetic reactions in a subcompartment of the endoplasmic reticulum, J. Biol. Chem. 274 (1999) 15203–15212.
[19] M.J. McConville, A.K. Menon, Recent developments in the cell biology and biochemistry of glycosylphosphatidylinositol lipids, Mol. Membr. Biol. 17 (2000) 1–16.
[20] N. Singh, L.N. Liang, M.L. Tykocinski, A.M. Tartakoff, A novel class of cell surface glycolipids of mammalian cells. Free glycosyl phosphatidylinositols, J. Biol. Chem. 271 (1996) 12879–12884.
[21] N.A. Baumann, J. Vidugiriene, C.E. Machamer, A.K. Menon, Cell surface display and intracellular trafficking of free glycosylphosphatidylinositols in mammalian cells, J. Biol. Chem. 275 (2000) 7378–7389.
[22] G. Arreaza, K.A. Melkonian, M. LaFevre-Bernt, D.A. Brown, Triton X-100-resistant membrane complexes from cultured kidney epithelial cells contain the Src family protein tyrosine kinase p62yes, J. Biol. Chem. 269 (1994) 19123–19127.
[23] D. Sevlever, S. Pickett, K.J. Mann, K. Sambamurti, M.E. Medof, T.L. Rosenberry, Glycosylphosphatidylinositol anchor intermediates associate with Triton insoluble membranes in subcellular

compartments that include the endoplasmic reticulum, Biochem. J. 343 (1999) 627–635.
[24] V.L. Stevens, H. Zhang, M. Harreman, Isolation and characterization of a Chinese hamster ovary (CHO) mutant defective in the second step of glycosyl-phosphatidylinositol biosynthesis, Biochem. J. 313 (1996) 253–258.
[25] K.J. Mann, M.R. Hepworth, N.S. Raikwar, M.A. Deeg, D. Sevlever, Effect of glycosylphosphatidylinositol (GPI)-phospholipase D overexpression on GPI metabolism, Biochem. J. 378 (2004) 641–648.
[26] V.L. Stevens, H. Zhang, Coenzyme A dependence of glycosylphosphatidylinositol biosynthesis in a mammalian cell-free system, J. Biol. Chem. 269 (1994) 31397–31403.
[27] T. Kawarabayashi, M. Shoji, L.H. Younkin, L. Wen-Lang, D.W. Dickson, T. Murakami, E. Matsubara, K. Abe, K.H. Ashe, S.G. Younkin, Dimeric amyloid beta protein rapidly accumulates in lipid rafts followed by apolipoprotein E and phosphorylated tau accumulation in the Tg2576 mouse model of Alzheimer's disease, J. Neurosci. 24 (2004) 3801–3809.
[28] E. London, D.A. Brown, Insolubility of lipids in triton X-100: physical origin and relationship to sphingolipid/cholesterol membrane domains (rafts), Biochim. Biophys. Acta 1508 (2000) 182–195.
[29] T. Kinoshita, K. Ohishi, J. Takeda, GPI-anchor synthesis in mammalian cells: genes, their products, and a deficiency, J. Biochem. (Tokyo) 122 (1997) 251–257.
[30] A. Pottekat, A.K. Menon, Subcellular localization and targeting of *N*-acetylglucosaminyl phosphatidylinositol de-*N*-acetylase, the second enzyme in the glycosylphosphatidylinositol biosynthetic pathway, J. Biol. Chem. 279 (2004) 15743–15751.
[31] M.E. Linder, R.J. Deschenes, New insights into the mechanisms of protein palmitoylation, Biochemistry 42 (2003) 4311–4320.
[32] V.L. Stevens, C.R.H. Raetz, Defective glycosyl phosphatidylinositol biosynthesis in extracts of three Thy-1 negative lymphoma cell mutants, J. Biol. Chem. 266 (1991) 10039–10042.
[33] S. Hirose, L. Ravi, S.V. Hazra, M.E. Medof, Assembly and deacetylation of *N*-acetylglucosaminyl-plasmanylinositol in normal and affected paroxysmal nocturnal hemoglobinuria cells, Proc. Natl. Acad. Sci. USA 88 (1991) 3762–3766.
[34] S. Hirose, L. Ravi, G.M. Prince, M.G. Rosenfeld, R. Silber, S.W. Andresen, S.V. Hazra, M.E. Medof, Synthesis of mannosylglucosaminylinositol phospholipids in normal but not paroxysmal nocturnal hemoglobinuria cells, Proc. Natl. Acad. Sci. USA 89 (1992) 6025–6029.
[35] D. Sevlever, D.R. Humphrey, T.L. Rosenberry, Compositional analysis of glucosaminyl(acyl)phosphatidylinositol accumulated in HeLa S3 cells, Eur. J. Biochem. 233 (1995) 384–394.
[36] T.L. Doering, W.J. Masterson, P.T. Englund, G.W. Hart, Biosynthesis of the glycosyl phosphatidylinositol membrane anchor of the trypanosome variant surface glycoprotein. Origin of the non-acetylated glucosamine, J. Biol. Chem. 264 (1989) 11168–11173.
[37] S. Ilangumaran, D.C. Hoessli, Effects of cholesterol depletion by cyclodextrin on the sphingolipid microdomains of the plasma membrane, Biochem. J. 335 (1998) 433–440.